

Twin-Layer RIS-Aided Differential Index Modulation Dispensing With Channel Estimation

Zhenyu Xiao, *Senior Member, IEEE*, Guangyao Liu, Tianqi Mao, *Member, IEEE*,
Ruiqi Liu, *Member, IEEE*, Wei Zhang, *Fellow, IEEE*, Xiang-Gen Xia, *Fellow, IEEE*,
and Lajos Hanzo, *Life Fellow, IEEE*

Abstract—In this correspondence, we propose a twin-layer hierarchical differential index modulation scheme for a reconfigurable intelligent surface (RIS)-aided transmitter architecture, termed as HD-RIS-IM. More specifically, the RIS array is partitioned into perfectly tiling sub-arrays. Each sub-array is mapped across multiple time slots, where each RIS element is activated only once at a particular time slot. These sub-arrays represented by sub-matrices are then used for constructing a block-based permutation matrix for data transmission. With the aid of this hierarchical structure, additional information can be conveyed by the specific order of the sub-arrays that are activated. Furthermore, extra bits are also embedded in the particular order of the RIS elements that are activated within each sub-array. By exploiting all the distinct permutations of the activated matrices, a differential modulation scheme is proposed for the RIS-aided transmitter, which maintains an M -ary phase shift keying (MPSK) and facilitates CSI-free demodulation. Furthermore, at the receiver, we propose a low-complexity distributed maximum likelihood (ML) detector, which significantly reduces the detection complexity. Our simulation results demonstrate the performance benefits of the proposed HD-RIS-IM scheme.

Index Terms—Index modulation (IM), reconfigurable intelligent surface (RIS), differential modulation, metasurface (MTS), intelligent reflecting surface (IRS).

I. INTRODUCTION

MULTIPLE-INPUT multiple-output (MIMO) techniques constitute a pivotal solution in support of high-rate data

This work was supported in part by the National Natural Science Foundation of China (NSFC) under grant numbers U22A2007 and 62171010, in part by Young Elite Scientists Sponsorship Program by CAST under Grant 2022ON-RCO01, and in part by Postdoctoral Science Foundation of China under Grant 2022M720361 and 2023T160040. L. Hanzo would like to acknowledge the financial support of the Engineering and Physical Sciences Research Council projects EP/W016605/1, EP/X01228X/1 and EP/Y026721/1 as well as of the European Research Council's Advanced Fellow Grant QuantCom (Grant No. 789028) (*Corresponding author: Tianqi Mao.*)

Copyright (c) 2015 IEEE. Personal use of this material is permitted. However, permission to use this material for any other purposes must be obtained from the IEEE by sending a request to pubs-permissions@ieee.org.

G. Liu, T. Mao and Z. Xiao are with the School of Electronic and Information Engineering, Beihang University, Beijing 100191, China (e-mail: {liugy, maotq, xiaozy}@buaa.edu.cn).

R. Liu is with the Wireless Research Institute, ZTE Corporation, Beijing 100029, China (e-mail: richie.leo@zte.com.cn).

Wei Zhang is with the School of Electrical Engineering and Telecommunications, University of New South Wales, Sydney, NSW 2052, Australia (e-mail: w.zhang@unsw.edu.au).

Xiang-Gen Xia is with the Department of Electrical and Computer Engineering, University of Delaware, Newark, DE 19716, USA (e-mail: xianggen@udel.edu).

L. Hanzo is with the School of Electronics and Computer Science, University of Southampton, Southampton SO17 1BJ, UK. (e-mail: lh@ecs.soton.ac.uk).

transmission, thanks to their superior multiplexing/diversity gains [1, 2]. However, these benefits are attained at the cost of a large number of radio-frequency chains harnessed for capacity enhancement. This inevitably results in excessive hardware complexity and cost as well as power consumption [3–5].

To tackle this issue, reconfigurable intelligent surfaces (RIS) [6–10] may be harnessed for improving the MIMO transmitter design. The RISs are typically manmade surfaces of electromagnetic (EM) meta-material, which are composed of metallic radiating elements. These elements facilitate the real-time manipulation of the amplitude/phase of the reflected waves under external control. Given this capability, a RIS-aided RF-chain-free transmitter architecture is developed [11]. More specifically, by flexibly controlling the EM responses of the radiating elements, the RIS array lends itself to amplitude/phase modulation (APM), without the need for RF chains [12]. Thanks to these merits, the RIS-aided transmitter architecture is considered to be a promising choice for a plethora of applications, such as aerial/satellite communications [13]. However, this architecture is still facing challenges. Specifically, the inflexible amplitude adjustment and the limited number of quantized phase shift choices of the EM responses of RIS elements make the employment of high-order modulation quite cumbersome.

The family of index modulation (IM) techniques has attracted extensive attention due to their superior energy and spectral efficiencies [14–16]. In IM-based systems, extra bits can be embedded into the activation pattern of the different transmit entities, such as subcarriers, time slots (TSs) and antennas, which convey the conventional APM symbols [17–19]. By viewing the RIS elements as the transmit entities, the IM philosophy can also be incorporated into RISs, which allows us to circumvent the aforementioned complexity challenges. There have been some preliminary investigations of RIS-aided IM schemes. For example, Basar [20] proposed a suite of RIS-assisted schemes for improving signal quality. In [21], RISs and receive quadrature spatial modulation (RQSM) were intrinsically integrated by steering the I- and Q- components of the reflected signal to different receive antennas (RAs). Luo et al. [22] proposed a pair of RIS-assisted spatial modulation (SM) schemes for uplink communication and advocated the joint optimization of the transmit power allocation and the RIS reflection coefficients. The existing contributions, however, mainly assumed having perfect channel state information (CSI). This assumption may gradually become more unrealistic as the scale of the RIS array grows, because the pilot

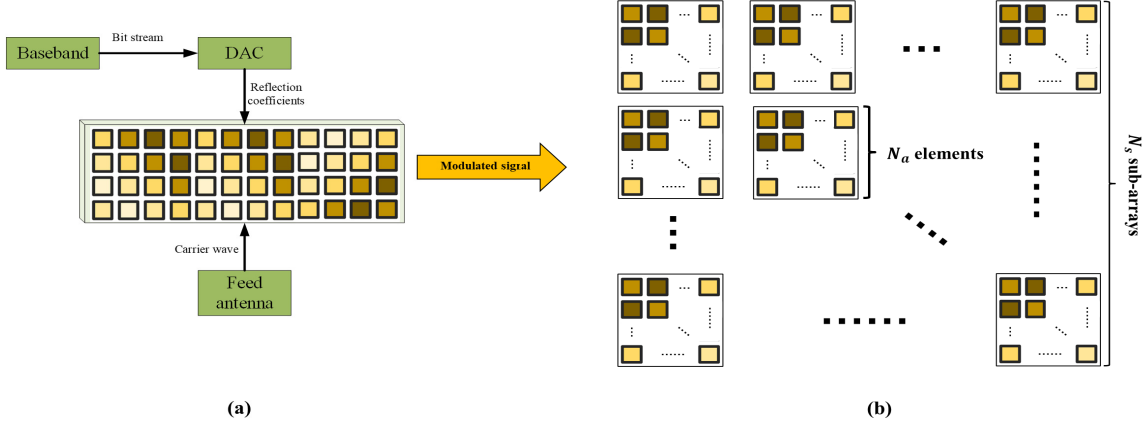


Fig. 1. (a) Architecture of RIS-aided transmitter. (b) Twin-layer hierarchical RIS array.

overhead required for accurate channel estimation becomes excessive.

Against this backdrop, in this correspondence, we propose a new twin-layer hierarchical differential RIS-aided index modulation (HD-RIS-IM) scheme.

- More specifically, the RIS array is partitioned into perfectly tiling sub-arrays, and each sub-array is mapped to a time block having multiple time slots. Then the activation indices of RIS reflecting elements (REs) and RIS sub-arrays are organized into two layers of indices to convey additional bits.
- By exploiting the permutations of both the sub-array indices and RIS element indices, we propose a differential modulation scheme for the RIS-aided transmitter, which maintains an M -ary phase shift keying (MPSK) signaling and facilitates CSI-free demodulation. Note that the proposed method applies to any arbitrary number of RIS elements.
- Furthermore, we propose a low-complexity distributed maximum likelihood (ML) detector, which converts the optimal ML matrix-based detector into distributed ML symbol-based detector, and hence substantially reduces the demodulation complexity. Our simulation results quantify the performance benefits of the proposed HD-RIS-IM scheme.

The rest of this correspondence is organized as follows. In Section II, we present the architecture of the RIS-aided transmitter. In Section III, we discuss both the proposed HD-RIS-IM scheme and the low-complexity distributed ML detector. Our simulation results and detailed discussions are provided in Section IV, while Section V concludes this compact letter.

II. SYSTEM MODEL

The generic architecture of our RIS-aided transmitter is shown in Fig. 1(a), where a RIS array composed of N reflecting elements (REs) is employed and the REs are arranged to form a two-dimensional structure. The bit stream is mapped to the RIS REs whose reflection coefficients are controlled by the external signal. On the other hand, the RIS array is irradiated by an unmodulated carrier provided by a feed

antenna. Explicitly, this single-tone carrier is fed uniformly to the REs through the air by the feed antenna. Then the reflected signal of the n -th RIS element can be written as

$$\tilde{P}_n = E_n e^{j\varphi_n} E_c e^{j2\pi f_c t}, n = 1, 2, \dots, N, \quad (1)$$

where f_c and E_c represent the frequency and amplitude of the single-tone carrier signal, respectively. Furthermore, φ_n and E_n denote the controllable phase and amplitude of the RE n , respectively, which can convey information bits through classical constellations, such as PSK. For instance, quadrature PSK (QPSK) can be readily realized by setting $E_n = 1$ and $\phi_n \in \{e^{j(0)}, e^{j(0.5\pi)}, e^{j(\pi)}, e^{j(1.5\pi)}\}$, where ϕ_n is determined by the input bits.

To enhance the energy efficiency of the RIS-aided transmitter, the specific activation pattern of the REs may be exploited for conveying extra information by relying on the IM philosophy. More specifically, only a fraction of the REs is activated for data transmission, whose indices can implicitly deliver additional information bits. Note that the existing RIS-aided IM schemes require accurate CSI estimate for demodulation [20–22], which can only be provided at the cost of a significant pilot overhead, which escalates upon increasing the number of REs. We next propose the HD-RIS-IM scheme by performing index modulation in a hierarchical and differential manner, where the CSI knowledge is no longer required for information recovery.

III. PROPOSED HD-RIS-IM SCHEME

A. Twin-Layer Hierarchical Index Modulation

Again, differential encoding based IM is capable of facilitating CSI-free demodulation, which can be realized for example by relying on the space-time block coding concept [23]. Inspired by this philosophy, a space-time (ST) transmit block \mathbf{S} is constructed by mapping the $N \times 1$ transmit vector of the RIS array to N TSs. To facilitate differential encoding, the set G containing all possible realizations of \mathbf{S} can be designed to meet the following constraints [23]:

$$\begin{cases} \forall \mathbf{S}_1, \mathbf{S}_2 \in G, \mathbf{S}_1 \mathbf{S}_2 \in G, \\ \|\mathbf{S}_1\|_F^2 = \|\mathbf{S}_2\|_F^2 = \|\mathbf{S}_1 \mathbf{S}_2\|_F^2, \end{cases} \quad (2)$$

where $\|\cdot\|_F^2$ denotes the Frobenius norm. Note that if \mathbf{G} consists of unitary matrices, (2) is satisfied and there were studies on unitary space-time block code designs for space-time differential modulations in the literature, such as [24]. To this end, a hierarchical IM scheme is tailored for the RIS array architecture considered, which is seen in Fig. 1(b). More specifically, the RIS array of size N is equally partitioned into N_s sub-arrays of N_a REs. During each of the N consecutive TSs, m bits are modulated as an $(N_a N_s) \times (N_a N_s)$ ST block \mathbf{X} , where the (e, t) th element denotes the symbol mapped to the RE e in TS t . This ST block \mathbf{X} can be designed as follows:

- **Index Layer 1:** During the transmission of \mathbf{X} , N consecutive TSs constitute N_s non-overlapping time blocks in total. In each time block, i.e. N_a consecutive TSs, only one out of N_s sub-arrays is activated for data transmission, whose index is determined by the specific incoming bits. Then additional information can be conveyed by the specific order of the N_s sub-arrays that are activated, termed as the sub-array activation pattern (SAP).
- **Index Layer 2:** Let us assume that the i -th sub-array is activated during the time block n for $n = 1, 2, \dots, N_s$. Then each RE of the i -th sub-array is activated once and only once in a TS within the time block n , whose index also depends on the incoming bits. By conceiving this arrangement, extra bits are also conveyed by the particular order of the REs that are activated within each sub-array. This is termed as an element activation pattern (EAP).
- Constant modulus PSK symbols are transmitted by the non-zero entries of \mathbf{X} . We denote the set of all these ST blocks \mathbf{X} as G_{perm} .

With this twin-layer hierarchical structure, each ST block $\mathbf{X} \in G_{perm}$ is unitary and thus $\|\mathbf{X}\|_F^2 = N_a N_s$ and \mathbf{X} satisfies (2). Furthermore, the total number of bits conveyed by each transmit block can be expressed as

$$m = m_1 + m_2 + m_3 \quad (3)$$

$$= \lfloor \log_2(N_s!) \rfloor + N_s \lfloor \log_2(N_a!) \rfloor + N_a N_s \log_2(M),$$

where $\lfloor \cdot \rfloor$ denotes the floor operation. In (3), $m_1 = \lfloor \log_2(N_s!) \rfloor$ and $m_2 = N_s \lfloor \log_2(N_a!) \rfloor$ represent the index bits (IB) conveyed by the SAPs and EAPs in each transmit block, respectively. Moreover, $m_3 = N_a N_s \log_2(M)$ stands for the number of classical data symbol bits modulated as M -ary PSK (MPSK) signals. If the N signals of REs are taken from different PSK constellations, say M_1 PSK, \dots , M_N PSK, respectively, then (3) can be readily generalized as

$$m = m_1 + m_2 + m_3 \quad (4)$$

$$= \lfloor \log_2(N_s!) \rfloor + N_s \lfloor \log_2(N_a!) \rfloor + \sum_{i=1}^N \log_2(M_i).$$

The specific orders of sub-arrays and REs that are activated and the m_1 -bits and m_2 -bits represent a unique and unambiguous one-to-one mapping. A pair of lookup tables are created for representing the corresponding permutations.

For explicitly visualizing the principle of the proposed twin-layer hierarchical IM scheme, an example considering $N_a = 3$ and $N_s = 3$ is provided in Fig. 2. The index mapping between the IB for SAP (IB-SAP) and SAP is: (a) IB-SAP = [0 0], SAP

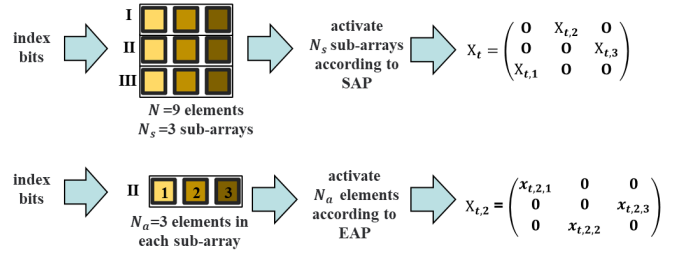


Fig. 2. An example for hierarchical index modulation.

TABLE I
THE INDEX MAPPING BETWEEN THE IB-SAP AND SAP FOR $N_s = 3$.

IB-SAP	SAP	\mathbf{X}_t
00	(1 2 3)	$\mathbf{X}_t = \begin{pmatrix} \mathbf{X}_{t,1} & 0 & 0 \\ 0 & \mathbf{X}_{t,2} & 0 \\ 0 & 0 & \mathbf{X}_{t,3} \end{pmatrix}$
01	(1 3 2)	$\mathbf{X}_t = \begin{pmatrix} \mathbf{X}_{t,1} & 0 & 0 \\ 0 & 0 & \mathbf{X}_{t,3} \\ 0 & \mathbf{X}_{t,2} & 0 \end{pmatrix}$
10	(2 1 3)	$\mathbf{X}_t = \begin{pmatrix} 0 & \mathbf{X}_{t,2} & 0 \\ \mathbf{X}_{t,1} & 0 & 0 \\ 0 & 0 & \mathbf{X}_{t,3} \end{pmatrix}$
11	(2 3 1)	$\mathbf{X}_t = \begin{pmatrix} 0 & 0 & \mathbf{X}_{t,3} \\ \mathbf{X}_{t,1} & 0 & 0 \\ 0 & \mathbf{X}_{t,2} & 0 \end{pmatrix}$

= (1 2 3); (b) IB-SAP = [0 1], SAP = (1 3 2); (c) IB-SAP = [1 0], SAP = (2 1 3); (d) IB-SAP = [1 1], SAP = (2 3 1). These are illustrated in Table I. Let us assume for example IB-SAP = [1 0] for the t th block. According to the index mapping, the t th block \mathbf{X}_t can be written in a partitioned matrix form as

$$\mathbf{X}_t = \begin{pmatrix} 0 & \mathbf{X}_{t,2} & 0 \\ \mathbf{X}_{t,1} & 0 & 0 \\ 0 & 0 & \mathbf{X}_{t,3} \end{pmatrix}, \quad (5)$$

where $\mathbf{X}_{t,i} \in \mathbb{C}^{N_a \times N_a}$ denotes the transmit sub-block of the i -th sub-array. The index mapping between IB for EAP (IB-EAP) and EAP for sub-array $\mathbf{X}_{t,2}$ is: (a) IB-EAP = [0 0], EAP = (1 2 3); (b) IB-EAP = [0 1], EAP = (1 3 2); (c) IB-EAP = [1 0], EAP = (2 1 3); (d) IB-EAP = [1 1], EAP = (2 3 1). Assuming that we have IB-EAP = [0 1], $\mathbf{X}_{t,2}$ can be formulated as

$$\mathbf{X}_{t,2} = \begin{pmatrix} x_{t,2,1} & 0 & 0 \\ 0 & 0 & x_{t,2,3} \\ 0 & x_{t,2,2} & 0 \end{pmatrix}, \quad (6)$$

where $x_{t,2,j}$ represents the M -PSK constellation symbols carried by the j th element activated in sub-array $\mathbf{X}_{t,2}$. For instance, if $M = 4$, i.e. QPSK is employed, $x_{t,2,j} \in \{e^{j(0)}, e^{j(0.5\pi)}, e^{j(\pi)}, e^{j(1.5\pi)}\}$, where $x_{t,2,j}$ is determined by the input bits.

B. Differential Transmission and Detection

Based on the proposed hierarchical structure of the transmit ST block, differential (de)modulation can be readily realized. The specific process is as follows.

- **Mapping:** At the HD-RIS-IM transmitter, each set of m incoming bits is mapped into \mathbf{X}_t according to the above

design, where we have $\mathbf{X}_t \in G_{perm}$. Specifically, the first m_1 bits are mapped to the SAP of the ST block. Then the next m_2 bits are mapped to the EAPs for all the sub-arrays. Finally, the remaining m_3 bits are mapped to the symbol drawn from the M -PSK alphabet. Based on the mapping results of the above three parts, \mathbf{X}_t can be determined.

- **Differential calculation:** Calculate the actual transmit block \mathbf{S}_t from \mathbf{X}_t in the following differential manner:

$$\mathbf{S}_t = \mathbf{S}_{t-1}\mathbf{X}_t, \quad (7)$$

where \mathbf{S}_t denotes the $(N_a N_s) \times (N_a N_s)$ block within the t -th $N_a N_s$ consecutive TSs and \mathbf{S}_0 is set as the identity matrix \mathbf{I} . Due to the permutation-based structure \mathbf{X} in our HD-RIS-IM design detailed above, all the transmission matrices \mathbf{S}_t in (7) also have a similar structure as \mathbf{X} , i.e. they obey $\mathbf{S}_t \in G_{perm}$ as well. This implies that the transmissions of the RIS REs are all MPSK signals even after differential modulation, i.e. the MPSK signaling patterns are retained. Therefore, the RIS REs at the transmitter do not have to change the phase set due to the differential calculation, once the modulation method has been determined.

- **Block transmission and reception:** After the differential calculation, the transmitter sends the block \mathbf{S}_t during N consecutive TSs.

Then the received signal corresponding to the t -th transmit block is given by

$$\mathbf{Y}_t = \mathbf{H}_t \mathbf{S}_t + \mathbf{Z}_t, \quad (8)$$

where the (i, j) th element of \mathbf{Y}_t represents the received signal of RA i at TS j , and \mathbf{H}_t denotes the $N_r \times N$ channel matrix. The (t, r) th entry of \mathbf{H}_t , represented by h_{tr} , denotes the path gain between the RE t and RA r . Here h_{tr} is modeled as a complex Gaussian variable with zero mean and unit variance, which is independent across different values of t and r . Besides, \mathbf{Z}_t stands for the $N_r \times 1$ AWGN matrix. Finally, N_r is the number of RAs.

1) *Maximum Likelihood Detector:* The ML detector considers all possible block realizations by searching for all possible signal constellation points and the activation orders of the sub-blocks and RIS REs.

According to (8), the signal received for the $(t+1)$ th ST block is then given by

$$\mathbf{Y}_{t+1} = \mathbf{H}_{t+1} \mathbf{S}_{t+1} + \mathbf{Z}_{t+1}. \quad (9)$$

We assume a quasi-static channel, where the fading coefficients remain constant over two adjacent ST blocks, i.e. $\mathbf{H}_{t+1} = \mathbf{H}_t$. Then, according to (7)-(9), \mathbf{Y}_{t+1} can be further written as

$$\mathbf{Y}_{t+1} = \mathbf{Y}_t \mathbf{X}_{t+1} - \mathbf{Z}_t \mathbf{X}_{t+1} + \mathbf{Z}_{t+1}. \quad (10)$$

The optimum ML detector is formulated as

$$\hat{\mathbf{X}}_t = \arg \min_{\mathbf{X} \in G_{perm}} \|\mathbf{Y}_t - \mathbf{Y}_{t-1} \mathbf{X}\|_F^2. \quad (11)$$

The total search complexity of the ML detector in (11) is on the order of $\mathcal{O}(2^{\lceil \log_2 N_s \rceil} 2^{N_s \lceil \log_2 N_a \rceil} M^{N_a N_s})$ per ST block.

2) *Low-Complexity Distributed Detector:* The complexity of the ML detector increases exponentially in terms of the signal constellation size M with the number of sub-arrays and REs. To tackle the escalating complexity, we propose a low-complexity distributed detector, which converts the above optimal ML matrix detector into a distributed optimal ML symbol detector.

At the receiver, \mathbf{Y}_t of (8) can be written as $\mathbf{Y}_t = [\mathbf{Y}_{t,1}, \dots, \mathbf{Y}_{t,N_s}]$, where $\mathbf{Y}_{t,i} \in \mathbb{C}^{N_r \times N_a}$. For a specific ST block \mathbf{X}_t , if the SAP is known, i.e. the order of the N_s sub-arrays that are activated is determined, $(\mathbf{Y}_t - \mathbf{Y}_{t-1} \mathbf{X})$ in (11) associated with $\mathbf{X} = \mathbf{X}_t$ can be rewritten as

$$\begin{aligned} & \mathbf{Y}_t - \mathbf{Y}_{t-1} \mathbf{X}_t \\ &= [\mathbf{Y}_{t,1}, \dots, \mathbf{Y}_{t,N_s}] - [\mathbf{Y}_{(t-1),p^1} \mathbf{X}_{t,p^1}, \dots, \mathbf{Y}_{(t-1),p^{N_s}} \mathbf{X}_{t,p^{N_s}}] \\ &= [\mathbf{Y}_{t,1} - \mathbf{Y}_{(t-1),p^1} \mathbf{X}_{t,p^1}, \dots, \mathbf{Y}_{t,N_s} - \mathbf{Y}_{(t-1),p^{N_s}} \mathbf{X}_{t,p^{N_s}}], \end{aligned} \quad (12)$$

where p^k denotes the index of the activated sub-array in the k th time block in \mathbf{X}_t and $k \in [1, 2, \dots, N_s]$. Then, upon assuming that the EAP for sub-array \mathbf{X}_{t,p^k} is known, i.e. the order of the N_a REs that are activated is determined, we may write $\mathbf{Y}_{t,k}$ as $\mathbf{Y}_{t,k} = [y_{t,k,1}, \dots, y_{t,k,N_a}]$, $y_{t,k,j} \in \mathbb{C}^{N_r \times 1}$. Hence we arrive at

$$\begin{aligned} & \mathbf{Y}_{t,k} - \mathbf{Y}_{(t-1),p^k} \mathbf{X}_{t,p^k} \\ &= [\dots, y_{t,k,i} - y_{(t-1),p^k,l^i} x_{t,p^k,l^i}, \dots], \end{aligned} \quad (13)$$

where l^i represents the index of the activated RE in the i th TS of the time block \mathbf{X}_{t,p^k} , $i \in [1, 2, \dots, N_a]$ and x_{t,p^k,l^i} represents the MPSK constellation symbol. Because $x_{t,p^1,l^1}, \dots, x_{t,p^{N_s},l^{N_a}}$ are independent of each other and they are all in different columns and different rows, they can be separately ML detected. Thus, in the k th time block, the i th symbol in \mathbf{X}_{t,p^k} can be optimally detected according to

$$\hat{x}_{t,p^k,l^i} = \arg \min_{\tilde{x}} \|y_{t,k,i} - y_{(t-1),p^k,l^i} \tilde{x}\|_F^2, \quad (14)$$

where \tilde{x} is chosen from the M -PSK constellation. For the \mathbf{X}_t whose SAP and EAPs are given, N data symbols can be detected by (14).

Therefore, the original optimal ML detector (11) is converted to the following distributed optimal ML symbol detector

$$\hat{\mathbf{X}}_t = \arg \min_{\substack{\text{SAP} \in \mathcal{N}_s \\ \& \text{EAPs} \in \mathcal{N}_a \\ \& \forall x_{t,p^1,l^1}, \dots, x_{t,p^{N_s},l^{N_a}}}} \|\mathbf{Y}_t - \mathbf{Y}_{t-1} \mathbf{X}\|_F^2, \quad (15)$$

where \mathcal{N}_s and \mathcal{N}_a represent the sets containing all possible SAP and EAP, respectively, and the symbols $x_{t,p^1,l^1}, \dots, x_{t,p^{N_s},l^{N_a}}$ are detected via (14).

The search complexity order of the proposed distributed detector is $\mathcal{O}(2^{\lceil \log_2 N_s \rceil} 2^{\lceil \log_2 N_a \rceil} NM)$ per ST block, clearly, this complexity increases linearly with the number of signal constellation points M . The proposed detector exploits the fact that each transmitted symbol of the ST block is related to one symbol of the previous ST block only, not to a whole block. By doing so, the complexity becomes roughly proportional to the number of transmitter antennas only. The above detection eliminated the excessive ML-detection complexity, yet, it is still the optimal ML detector for each transmitted symbol.

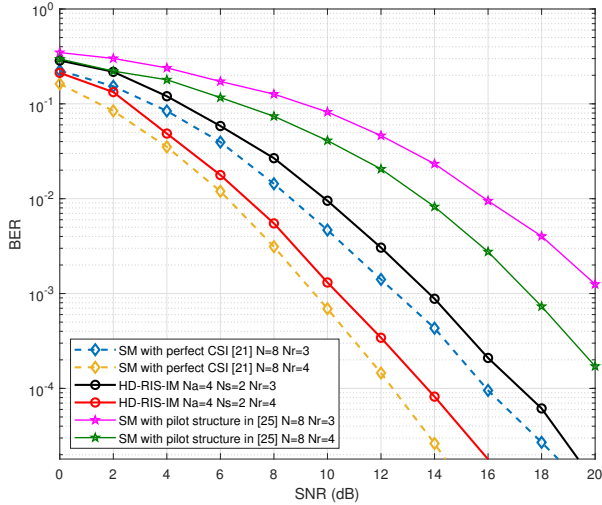


Fig. 3. BER performance comparison between the proposed HD-RIS-IM and classical SM at 4 bits/s/Hz, where $N=8$ and $N_r=2,3,4$.

Therefore, the proposed distributed detector has the same performance as the ML detector.

As a reference, the computational complexity of the proposed HD-RIS-IM and of the existing SM/differential SM (DSM) schemes is compared. Within the duration of a space-time block, the search complexity of the optimal detector used for the classical SM is $\mathcal{O}(N^2M)$ [21]. Furthermore, the search complexity of the optimal detector used for the DSM schemes is $\mathcal{O}(2^{\lceil \log_2 N! \rceil} M^N)$ [25], which increases exponentially with N and $\log_2 N!$. On the other hand, the search complexity of the proposed HD-RIS-IM is calculated to be $\mathcal{O}(2^{\lceil \log_2 N_s! \rceil} 2^{\lceil \log_2 N_a! \rceil} NM)$, which increases linearly with M . Therefore, the proposed HD-RIS-IM exhibits its superiority over the DSM in terms of receiver complexity, which is on the same order of the classical SM.

IV. SIMULATION RESULTS AND ANALYSIS

In this section, our bit error rate (BER) simulation results are presented for evaluating the performance of the proposed HD-RIS-IM system under various system configurations, where the proposed low-complexity distributed detector is utilized. The classical SM, DSM and Alamouti schemes are also simulated as benchmarks, where ML detection is utilized.

Fig. 3 shows our BER performance comparison versus the signal-to-noise ratio (SNR) at the receiver between the proposed HD-RIS-IM and the conventional SM scheme [21]. The numbers of REs and RAs are set to $N = 8$ and $N_r = 2, 3, 4$, respectively. The RIS REs are divided into two groups in HD-RIS-IM, i.e., $N_a = 4$, $N_s = 2$. The spectral efficiency is fixed to 4 bits/s/Hz. Then BPSK can be employed in the classical SM with perfect CSI, whilst HD-RIS-IM uses 8PSK for the first seven TSs and 8PSK for the last TS in each time block to reach the same spectral efficiency. We also considered SM using the pilot structure in [25], where the pilot symbols \mathbf{P} obey $\mathbf{P} = \mathbf{I}_N$. Therefore, the data within each SM frame can be represented as $x_{SM} = [\mathbf{P} \ x_{data}]$. The durations

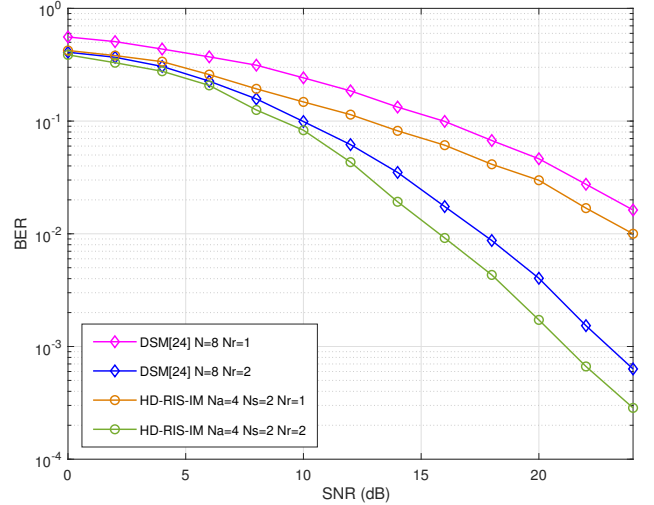


Fig. 4. BER performance comparison between the proposed HD-RIS-IM and DSM at 4 bits/s/Hz, where $N=8$ and $N_r=1,2$.

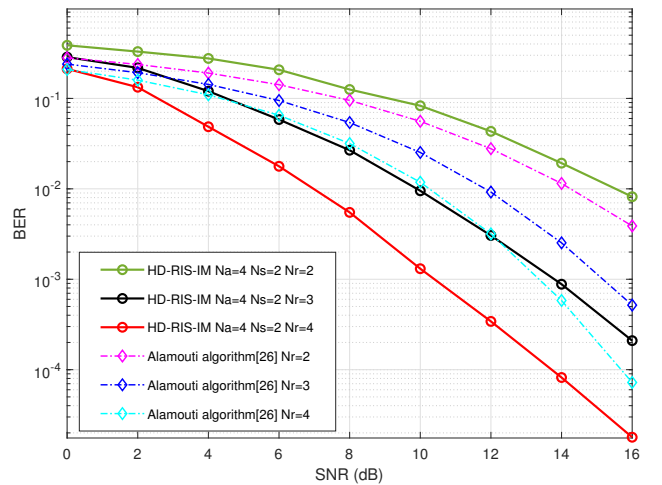


Fig. 5. BER performance of the proposed HD-RIS-IM with $N=8$ versus Alamouti scheme at 4 bits/s/Hz transmission rate, where $N_r=2,3,4$.

of pilots, and the whole frame data are N TSs and $2N$ TSs, respectively, in order to closely approach the performance of perfect channel estimation. In this frame structure, 32-PSK is employed in the SM to reach the spectral efficiency of 4 bits/s/Hz. It can be observed that at BER values of about 10^{-3} , the HD-RIS-IM scheme has an SNR loss from 1 dB to 2 dB ranging in comparison to SM with perfect CSI. This can be explained by the fact that the HD-RIS-IM scheme uses a higher modulation order than SM to reach for the spectral efficiency of 4 bits/s/Hz. In comparison to SM using the pilot structure of [25], HD-RIS-IM exhibits significant performance advantages because the SM uses higher modulation order to make up for its spectral efficiency loss caused by the pilot overhead. And the spectral efficiency advantages of HD-RIS-IM will become increasingly further as the scale of the RIS array grows.

Fig. 4 shows our BER performance comparison between the proposed HD-RIS-IM and DSM [24], where we have $N = 8$, $N_a = 4$, $N_s = 2$, and $N_r = 1, 2$. The spectral efficiency of both schemes is set to 4 bits/s/Hz. DSM uses QPSK for the first seven TSs and 8-PSK for the last TS in each time block, whilst the same QPSK plus 8-PSK strategy, as in Fig. 3 is employed in HD-RIS-IM. It can be observed that HD-RIS-IM exhibits better performance than DSM for $N_r = 1, 2$. This is because the time domain isolation between different subblocks for HD-RIS-IM can reduce the probability of wrong ST block detection, leading to a lower BER level. Therefore, the proposed HD-RIS-IM is considered a preferable choice over the classical DSM for practical applications.

In Fig. 5, we investigate the performance of HD-RIS-IM versus the differential scheme of the well-known Alamouti algorithm [26] with a fixed spectral efficiency of 4 bits/s/Hz. 16-PSK is employed in the Alamouti scheme, whilst HD-RIS-IM uses the same QPSK plus 8-PSK strategy as above. It can be observed from Fig. 5 that, HD-RIS-IM suffers from a performance loss when $N_r = 2$. This is because when the number of RAs is small, the BER of HD-RIS-IM is dominated by the erroneous estimation of EAP and SAP, which diminish the throughput gain of index bits. As the number of RAs increases, the erroneous symbol detection gradually dominates the BER of HD-RIS-IM. Therefore, the HD-RIS-IM begins to outperform Alamouti algorithm in the case of $N_r = 3, 4$ as a benefit of using lower-order modulation.

V. CONCLUSIONS

In this correspondence, we have proposed a twin-layer hierarchical differential IM scheme for RIS-aided communications, whose differential structure implicitly carries additional bits by the permutation patterns of both the sub-matrices and the RIS REs. As a benefit, the MPSK signal patterns can be retained for RIS transmission after the differential operation, and no CSI is needed at the receiver. Furthermore, we have proposed a low-complexity distributed ML detector based on the proposed hierarchical structure. Our simulation results revealed that channel estimation can be dispensed with the benefit of the proposed method, which is achieved at an SNR degradation of less than 3 dB compared to SM with perfect CSI. And the proposed method exhibits significant performance advantages compared to the SM taking the CSI overhead into account. It is also noted that the proposed HD-RIS-IM scheme exhibits a performance gain over conventional DSM and Alamouti schemes.

REFERENCES

- [1] Y. Wu, C. Xiao, Z. Ding, X. Gao, and S. Jin, "A survey on MIMO transmission with finite input signals: Technical challenges, advances, and future trends," *Proc. IEEE*, vol. 106, no. 10, pp. 1779–1833, Jul. 2018.
- [2] E. Al Abbas, M. Ikram, A. T. Mobashsher, and A. Abbosh, "MIMO antenna system for multi-band millimeter-wave 5G and wideband 4G mobile communications," *IEEE Access*, vol. 7, pp. 181916–181923, Dec. 2019.
- [3] T. Gong, N. Shlezinger, S. S. Ioushua, M. Namer, Z. Yang, and Y. C. Eldar, "RF chain reduction for MIMO systems: A hardware prototype," *IEEE Syst. J.*, vol. 14, no. 4, pp. 5296–5307, Mar. 2020.
- [4] N. Shlezinger, Y. C. Eldar, and M. R. Rodrigues, "Asymptotic task-based quantization with application to massive MIMO," *IEEE Trans. Signal Process.*, vol. 67, no. 15, pp. 3995–4012, Jun. 2019.
- [5] J. Zhu, W. Xu, and N. Wang, "Secure massive MIMO systems with limited RF chains," *IEEE Trans. Veh. Technol.*, vol. 66, no. 6, pp. 5455–5460, Oct. 2016.
- [6] X. Chen, J. C. Ke, W. Tang, M. Z. Chen, J. Y. Dai, E. Basar, S. Jin, Q. Cheng, and T. J. Cui, "Design and implementation of MIMO transmission based on dual-polarized reconfigurable intelligent surface," *IEEE Wirel. Commun. Lett.*, vol. 10, no. 10, pp. 2155–2159, Oct. 2021.
- [7] E. Basar, M. Di Renzo, J. De Rosny, M. Debbah, M.-S. Alouini, and R. Zhang, "Wireless communications through reconfigurable intelligent surfaces," *IEEE Access*, vol. 7, pp. 116753–116773, Aug. 2019.
- [8] R. Liu, Q. Wu, M. Di Renzo, and Y. Yuan, "A path to smart radio environments: An industrial viewpoint on reconfigurable intelligent surfaces," *IEEE Wirel. Commun.*, vol. 29, no. 1, pp. 202–208, Jan. 2022.
- [9] R. Liu, J. Dou, P. Li, J. Wu, and Y. Cui, "Simulation and field trial results of reconfigurable intelligent surfaces in 5G networks," *IEEE Access*, vol. 10, pp. 122786–122795, Nov. 2022.
- [10] M. Jian, G. C. Alexandropoulos, E. Basar, C. Huang, R. Liu, Y. Liu, and C. Yuen, "Reconfigurable intelligent surfaces for wireless communications: Overview of hardware designs, channel models, and estimation techniques," *Intell. Converged Netw.*, vol. 3, no. 1, pp. 1–32, Mar. 2022.
- [11] W. Tang, M. Z. Chen, J. Y. Dai, Y. Zeng, X. Zhao, S. Jin, Q. Cheng, and T. J. Cui, "Wireless communications with programmable metasurface: New paradigms, opportunities, and challenges on transceiver design," *IEEE Wirel. Commun.*, vol. 27, no. 2, pp. 180–187, Apr. 2020.
- [12] Z. Zhou, N. Ge, Z. Wang, and L. Hanzo, "Joint transmit precoding and reconfigurable intelligent surface phase adjustment: A decomposition-aided channel estimation approach," *IEEE Trans. Commun.*, vol. 69, no. 2, pp. 1228–1243, Oct. 2020.
- [13] Z. Xiao, J. Yang, T. Mao, C. Xu, R. Zhang, Z. Han, and X.-G. Xia, "LEO satellite access network (LEO-SAN) towards 6G: Challenges and approaches," *IEEE Wirel. Commun.*, early access, Dec. 2022, doi: 10.1109/MWC.011.2200310.
- [14] C. Xu, Y. Xiong, N. Ishikawa, R. Rajashekar, S. Sugiura, Z. Wang, S.-X. Ng, L.-L. Yang, and L. Hanzo, "Space-, time- and frequency-domain index modulation for next-generation wireless: A unified single-/multi-carrier and single-/multi-RF MIMO framework," *IEEE Trans. Wirel. Commun.*, vol. 20, no. 6, pp. 3847–3864, Feb. 2021.
- [15] S. D. Tusha, A. Tusha, E. Basar, and H. Arslan, "Multidimensional index modulation for 5G and beyond wireless networks," *Proc. IEEE*, vol. 109, no. 2, pp. 170–199, Dec. 2020.
- [16] S. Gopi, S. Kalyani, and L. Hanzo, "Coherent and non-coherent multi-layer index modulation," *IEEE Access*, vol. 7, pp. 79677–79693, Jun. 2019.
- [17] T. Mao, Q. Wang, Z. Wang, and S. Chen, "Novel index modulation techniques: A survey," *IEEE Commun. Surveys Tuts.*, vol. 21, no. 1, pp. 315–348, Jul. 2018.
- [18] N. Ishikawa, S. Sugiura, and L. Hanzo, "50 years of permutation, spatial and index modulation: From classic RF to visible light communications and data storage," *IEEE Commun. Surveys Tuts.*, vol. 20, no. 3, pp. 1905–1938, Mar. 2018.
- [19] M. Wen, B. Zheng, K. J. Kim, M. Di Renzo, T. A. Tsiftsis, K.-C. Chen, and N. Al-Dhahir, "A survey on spatial modulation in emerging wireless systems: Research progresses and applications," *IEEE J. Sel. Areas Commun.*, vol. 37, no. 9, pp. 1949–1972, Jul. 2019.
- [20] E. Basar, "Reconfigurable intelligent surface-based index modulation: A new beyond MIMO paradigm for 6G," *IEEE Trans. Commun.*, vol. 68, no. 5, pp. 3187–3196, May 2020.
- [21] J. Yuan, M. Wen, Q. Li, E. Basar, G. C. Alexandropoulos, and G. Chen, "Receive quadrature reflecting modulation for RIS-empowered wireless communications," *IEEE Trans. Veh. Technol.*, vol. 70, no. 5, pp. 5121–5125, May 2021.
- [22] S. Luo, P. Yang, Y. Che, K. Yang, K. Wu, K. C. Teh, and S. Li, "Spatial modulation for RIS-assisted uplink communication: Joint power allocation and passive beamforming design," *IEEE Trans. Commun.*, vol. 69, no. 10, pp. 7017–7031, Oct. 2021.
- [23] Y. Bian, X. Cheng, M. Wen, L. Yang, H. V. Poor, and B. Jiao, "Differential spatial modulation," *IEEE Trans. Veh. Technol.*, vol. 64, no. 7, pp. 3262–3268, Jul. 2014.
- [24] B. L. Hughes, "Differential space-time modulation," *IEEE Trans. Inf. Theory*, vol. 46, no. 7, pp. 2567–2578, Nov. 2000.
- [25] S. Sugiura and L. Hanzo, "Effects of channel estimation on spatial modulation," *IEEE Signal Process. Lett.*, vol. 19, no. 12, pp. 805–808, Oct. 2012.
- [26] S. M. Alamouti, "A simple transmit diversity technique for wireless communications," *IEEE J. Sel. Areas Commun.*, vol. 16, no. 8, pp. 1451–1458, Oct. 1998.